Optimization of Plasma Production with Impedance Analysis for a Micro RF Ion Thruster

IEPC-2015-470p／ISTS-2015-b-470p

Kaito Nakagawa[1]
Yokohama National University, Tokiwadai 79-1, Hodogaya-ku Yokohama-shi, Kanagawa, 240-8501, Japan

Abstract: We investigate the conditions optimized generating plasma for micro RF ion thruster (mRIT) which has the discharge chamber that is one of the smallest size in the world. To search the optical conditions in priority to the speed, we calculate the simulation model that is composed of the equivalency circuit model and the global model. Since the global model has not been taken account into the calculate model for mRIT yet, so we first confirm the influences of this model. Then, we find that the electron density and temperature are varied, but the efficiency is almost not affected by the global model. From that point of the sheath thickness, we find that we cannot always ignore the sheath resistance on the chamber sidewall. Next we investigate the influence whether including this sheath resistance or not. If taken account of this sheath resistance, the efficiency is improved greatly in the lower RF frequency that is RF frequency is less than 100 MHz.

Nomenclature

ε_0	=	dielectric constant of vacuum
μ_0	=	magnetic permeability of vacuum
ω_{pe}	=	plasma frequency
ν_{me}	=	collision frequency between electron and neutral particle
ω	=	angular frequency
δ	=	skin depth of plasma
π	=	circular constant
d	=	thickness
$freq$	=	frequency of the power supplied amplitude of voltage
j	=	the imaginary unit
l	=	length of discharge chamber
r	=	radius of discharge chamber
n_e	=	electron density
T_e	=	electron temperature
u_B	=	Bohm velocity
P	=	power
I	=	current
Z	=	impedance
R	=	resistance
X	=	reactance
C	=	capacitance
L	=	inductance

Subscripts

[1] Graduated student, Department of Mechanical Engineering, E-mail:nakagawa-kaito-mf@ynu.jp.

abs = absorption
ind = inductive
cap = capacitive
sh1 = the sheath on the sidewall of the discharge chamber
sh2 = the sheath on the ground of the discharge chamber

I. Introduction

Recntly microsatellites (less than 100 kg) have been attracting a lot of interest from the space engineering community. These microsatellites can be manufactured and operated by small organization, such as universities and small companies. However, because of the limit of weight, volume, and electric power, almost all of microsatellites do not have any propulsion system. Therefore, the development of high-performance microthrusters is needed for orbit control. Since ion thrusters are one of the most promising microthrusters, we have developed a micro RF ion thruster (mRIT) (Figure.1). The mRIT has the radius and the length of its discharge chamber which are 5 mm and 10 mm, and this is one of the smallest size in the world. It is advantaged that the mRIT does not have magnets or electrodes, so the mRIT is light and high reliability [1].

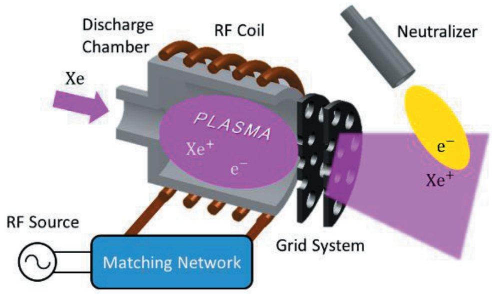

Figure 1. The schematic model of mRIT.

Owing to strong limitations lile above, the efficiency of plasma generation has to be high level. Whereas RF ion thrusters which are normally size have already studied by experimentally or numerically analysis, this mRIT has not studied adequately yet. This study is investigated what the conditions for which plasma is generated is to realize the high efficiency operation in mRIT. In this study, we analyze the characteristic of the plasma by numerical methods. Although there are some methods which the state of plasma is calculated, here, setting highly valued on the calculate speed for the roughly searching the optimized condition, we use the method of the equivalency circuit model and the global model which are superior in speed.

In the present study, by these models, we investigate the plasma absorbed power and the plasma impedance which depend on the RF frequency and neutral gas pressure. At this stage, because we have not done the experiment, we have not compared the numerical results to the experimental results, yet. That is left for the future work.

II. Assumption

For simplifying the model, we assume like below.

- Only Xe ions and electrons are treated as particles, and the ion species of interest is singly-ionized Xe^+ only.
- Neutral particles have Maxwellian velocity distribution at the gas temperature of 300 K.
- The reactions between electrons and neutral particles taken into account are elastic scattering, excitation, and ionization for electrons, and elastic scattering and charge exchange for ions, as below.

$$e^- + Xe \rightarrow e^- + Xe \qquad \text{(Elastic Scattering)}$$
$$e^- + Xe \rightarrow e^- + Xe^* \qquad \text{(Excitation)}$$
$$e^- + Xe \rightarrow e^- + Xe^+ + e^- \qquad \text{(Ionization)}$$

- The motion of excited-state atoms and ions is not considered.
- Coulomb collisions are not taken into account.
- The sheath model is the Child-Langmuir model and the electron density in bulk plasma is different from at sheath edge.

III. Equivalency Circuit Model

It is known that inductive discharge has two discharge modes, which are H-mode in which the inductive coupling plasma (ICP) is produced and E-mode in which the capacitive coupling plasma (CCP) is produced [2)]. The simplified model of inductive discharge is figure.2. Each mode is independent. Hence, to investigate the characteristic of plasma which is produced in inductive discharge, the equivalency circuit model is had to include the parallel circuit which is made these modes (figure.3).

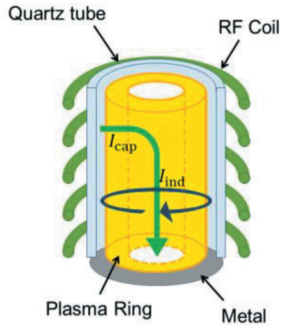

Figure 2. The schematic of inductive discharge.

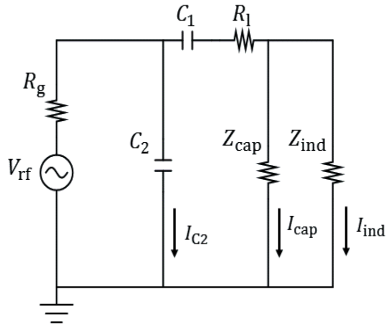

Figure 3. The whole circuit model.

A. ICP Circuit Model

In figure.4, ICP circuit correspond to the current around the plasma ring. The primary coil of the transformer is the induction coil, which is composed of N turns with inductance L_{coil} and resistance R_{coil} . The equivalent inductive circuit model is figure.5.The plasma is assumed to be one-turn secondary winding of hollo induction coil with inductance $L_1 + L_{e1}$ and resistanceR_{p1}. The plasma inductance is composed of two components, the geometrical inductance L_1 due to the plasma current path, and the electron inertia inductance L_{e1}. The mutual induction between the primary and secondary coil is represented by the mutual inductance M.

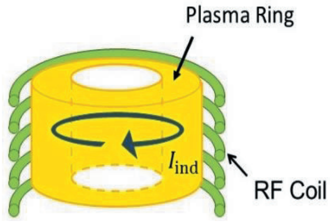

Figure 4. The schematic of ICP model.

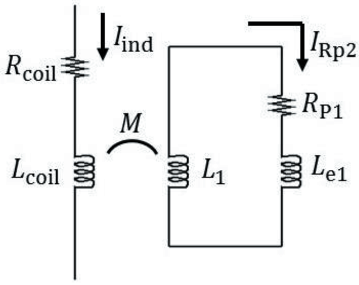

Figure 5. The ICP circuit.

The electric properties of plasma are described by the plasma conductivity.

$$\sigma_p = \frac{\varepsilon_0 \omega_{pe}^2}{\nu_{me} + j\omega} \tag{1}$$

The plasma resistance is defined by the real part of plasma conductivity

$$R_{p1} = \mathrm{Re}\left[\frac{1}{\sigma_p}\right] \cdot \frac{l_{path1}}{A_{path1}} \tag{2}$$

Where l_{path1} and A_{path1} are the length and cross sectional area of the plasma current path in ICP. Likewise, the plasma reactance is defined by the imaginary part of plasma conductivity

$$X_{e1} = \mathrm{Re}\left[\frac{1}{\sigma_p}\right] \cdot \frac{l_{path1}}{A_{path1}}, \tag{3}$$

so, the plasma inductance is defined

$$L_{e1} = \frac{X_{coil}}{\omega}. \tag{4}$$

We assume that the current path in ICP is the center between the radius of chamber and the thickness of the plasma ring. The geometric inductance L_1 is due to the current path of the plasma ring

$$L_1 = \frac{\mu_0 \pi (r - \delta)^2}{l}. \tag{5}$$

The mutual inductance M is

$$M = k_M \sqrt{L_{coil} L_1}. \tag{6}$$

where k_M is the coupling coefficient.

The transformed circuit can be described as figure.6. Hence, the impedance of the transformer circuit Z_{ind} is

$$Z_{ind} = R_{coil} + j\omega L_{coil} + Z_p \quad (7)$$

where Z_p which is the impedance of the part of the parallel circuit in figure.6 is defined

$$\frac{1}{Z_p} = \frac{1}{j\omega M} + \frac{1}{j\omega(L_1 - M + L_{e1}) + R_{p1}}. \quad (8)$$

The absorbed power in ICP is defined

$$P_{ind} = (Z_{ind} I_{ind}) \cdot \tilde{I}_{ind}, \quad (9)$$

where I_{ind} is the current in the primary coil, $\tilde{I}_{ind}$ is the conjugate complex number of I_{ind}.

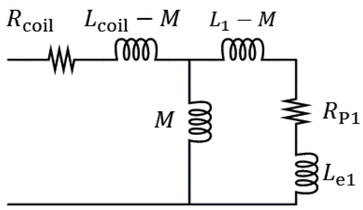

Figure 6. The transformed ICP circuit.

B. CCP Circuit Model

We assume that the current of CCP, I_{cap} is flowed, like figure.7, from high voltage coil to a ground through the quartz glass, cylindrical plasma and sheath. Capacitive coupling can be modeled as a series circuit. Figure.8 is the circuit model of CCP. In this circuit, C_q is the quartz capacitance, C_{sh1} is the sheath next to the quartz, R_{p2} is the plasma resistance due to ohmic heating, L_2 is the plasma inductance due to the electron inertia, C_{sh2} is the plasma-to-ground electrode sheath capacitance and R_{sh2} is the sheath resistance due to the collisionless stochastic process.

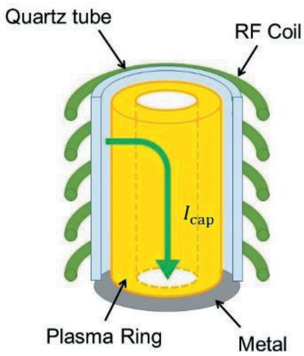

Figure 7. The schematic CCP model.

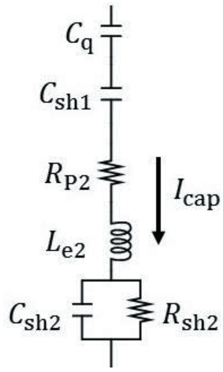

Figure 8. The CCP circuit model.

C. Matching Network

For RF circuits, maximizing deliverable power to a load is important issue. We consider a simplify circuit which has a load with the impedance $Z = R + jX$ and RF power source is V and internal resistance is R_g. The power consumption of the load is

$$P = \frac{V^2 R}{(R_g + R)^2 + X^2}. \quad (10)$$

If $R = R_g$ and $X = 0$, the power consumption is maximized to be $P = V^2/4R$. Then we consider matching the load impedance $Z_s = R_s + jX_s$ and the internal resistance R_g by L-shaped matching network (figure.9). Calculating the composed impedance, the variable capacitance C_1 and C_2 are determined to be

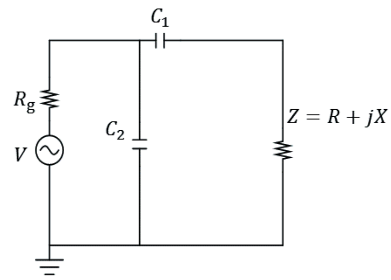

Figure 9. The matching network.

$$C_1 = \frac{1}{\omega\left(X_s - \sqrt{R_s R_g - R_s^2}\right)} \quad (11)$$

$$C_2 = \frac{\sqrt{R_s R_g - R_s^2}}{\omega R_s R_g}. \quad (12)$$

IV. Global Model

It is not adequately that the electron temperature and density which are primary physical quantity on plasma are calculated by the equivalency circuit model because in the circuit model, the electron temperature and density are fixed and not updated. However, taken into account for the global model, we can update the electron temperature and density. The global model is the equations related on energy and particle balance. Here, we assume the plasma is a steady state.

A. Energy Balance

When plasma exists in steady state, it is equal the plasma absorbed power P_{abs} and the plasma consume power P_{dis}. The absorbed power can be calculated in the equivalency circuit model. On the other hand, the consume power can be described below

$$P_{\mathrm{dis}} = e n_{\mathrm{e}} u_{\mathrm{B}} A_{\mathrm{eff}} \varepsilon_{\mathrm{tot}}, \tag{13}$$

where $A_{\mathrm{eff}} = 2\pi \mathrm{R}^2 h_{\mathrm{l}} + 2\pi R L h_r$ is the effective area foe the particle loss, ε_{tot} is the total energy loss per electron-ion pair from the system. We assume that the plasma loss is caused by the collision between electron and neutral particle and the electron and ion kinetic energy lost at a surface. With equation.13 and $P_{\mathrm{abs}} = P_{\mathrm{dis}}$, we obtained

$$n_{\mathrm{e}} = \frac{\mathrm{P_{abs}}}{e u_{\mathrm{B}} A_{\mathrm{eff}} \varepsilon_{\mathrm{tot}}}. \tag{14}$$

Thus, we can calculate the electron density.

B. Particle Balance

The variety of the number of electron in the system is described below [3)]

$$V \frac{d n_{\mathrm{e}}}{dt} = K_{\mathrm{iz}} n_{\mathrm{e}} n_{\mathrm{g}} V - n_{\mathrm{e}} u_B A_{\mathrm{eff}}, \tag{15}$$

where V is the volume of discharge chamber. The first term of the right side means a number of electron which is created in the system, and the second term means a number of electron which is disappointed in the system. Here, we assuming in steady state, the left side of this equation is zero. We assume that the electron velocity is the Maxwell distribution, so from the analogy to Arrhenius equation, K_{iz} is proportional to the electron temperature. Hence, relation of the particle balance is described

$$\frac{K_{\mathrm{iz}}}{u_{\mathrm{B}}} = \frac{A_{\mathrm{eff}}}{n_{\mathrm{g}} V}. \tag{16}$$

From equation.15, we can calculate the electron temperature in numerical.

V. Result and Discussion

Next, we describe the result of the calculation of this model. The condition is table.1. The power supply frequency and the pressure of the neutral gas is the variable, the analysis is carried out for the wide range of frequency $f = 1$-1000 MHz and pressure $p = 0.1$-10.0 Pa and the supplied power is 200 mW. The coupling coefficient is fixed 0.2 [4)].

Table 1. The calculate conditions.

Radius	5.0	mm
Length	10	mm
The number of coil winding	5	times
Thickness of dielectric	1.0	mm
The kind of propulsion	Xe	-

A. Evaluating Model of The Global Model

In the former study of mRIT, there is nothing that the model which is included the global model. So, first, we investigate the influence, taken account of the global model.

1. Electron Density and Temperature

Figure.10-13 show the electron density and temperature as functions of RF frequency and neutral gas pressure. Not with global model, we can confirm that the electron density and temperature do not have the dependency of the RF frequency nor neutral gas pressure. On the other hand, taken account of global model, it is clear that the density and temperature have the dependency except for the pair of the temperature and frequency. Furthermore, we find that the density has the maximum value at $p = 1.0$ Pa.

2. Impedance Frequency Characteristic

Figure.14 and 15 show the resistance and reactance of the discharge chamber and the transmission line as a function of RF frequency. At the lower frequency area which is lower than 100 MHz, the resistance and reactance with global model are no more than not with global model. On the other hand, at the higher frequency area which is higher than 100 MHz, it is different from the two conditions. And we find that the resistance has the dependency of neutral gas pressure with global model but hardly has the dependency not with. Conversely, we also find that the reactance does not have the dependency of the pressure with global model but has the dependency not with. By the way, there is a blank around 100 MHz. From equation.11, it is clear that the resistance of the discharge chamber and the transmission line must be lower than 50 Ω. So, we consider that the resistance is much more than 50 Ω in this area.

Next, figure.16 and 17 show the resistance and reactance of ICP as a function of frequency. There is no difference from the two conditions here. But from figure.18 and 19 which show the resistance and reactance of CCP, there is big difference. Especially not with global model, the resistance of CCP is almost constant with increasing RF frequency.

3. Absorbed Power and Efficiency

Figure.20 and 21 show the inductive and capacitive absorbed power as a function of RF frequency. From figure.20, whether with global model or not, the inductive absorbed power in the lower frequency is bigger than in the higher frequency. That is why, though from figure.16, the resistance of ICP in the higher frequency is bigger than in the lower frequency, the current through ICP in the higher frequency which figure.22 shows is much less than in the lower frequency. On the other hand, figure.21 show that the capacitive absorbed power in higher frequency is more than in lower frequency. However, because there is a big difference of orders between inductive and capacitive, the total absorbed power which figure.23 shows is dominated by the capacitive one.

Figure.24 shows the total absorbed efficiency as a function of RF frequency. We find that there is hardly a difference between the two conditions. If frequency is between 150-300 MHz, the efficiency is more than 95%. Because the power to the discharge chamber is kept being equal to the half of the supplied power due to matching network, the tendency of the efficiency against RF frequency is similar to that of the capacitive power absorbed.

4. Sheath

Figure.25 shows the sheath thickness on the wall of the discharge chamber. Not with global model, the sheath thickness do not depended on RF frequency because the electron density and temperature is fixed. While in the higher frequency there is not difference, in the lower frequency the maximum sheath thickness is about 2.5 mm and the sheath thickness on the ground which figure.26 shows have a similar tendency and the maximum thickness is about 2.0 mm. Because the radius and the half of the height of the discharge chamber are 5.0 mm, respectively, it is clear that the proportion of both the sheath thicknesses to the plasma is very large. Hence, the fact is we imply that in mRIT the circuit elements about sheath be not able to be ignored.

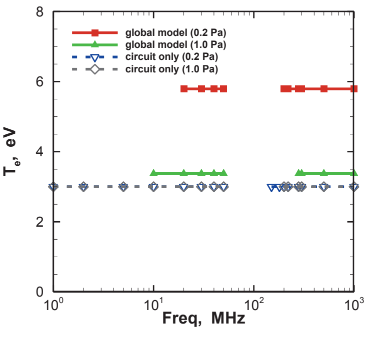

Figure 10. The electron temperature with frequency.

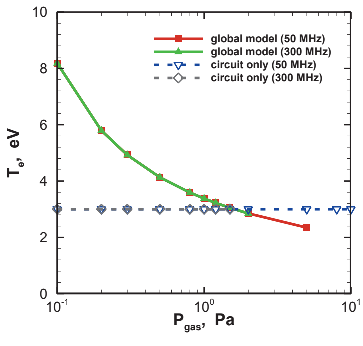

Figure 11. The electron temperature with neutral gas pressure.

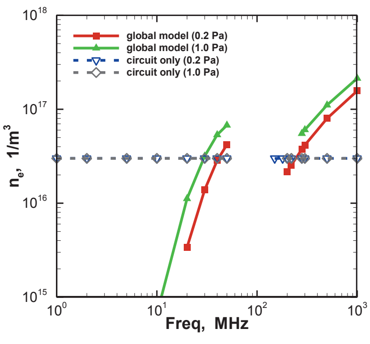

Figure 12. The electron density with frequency.

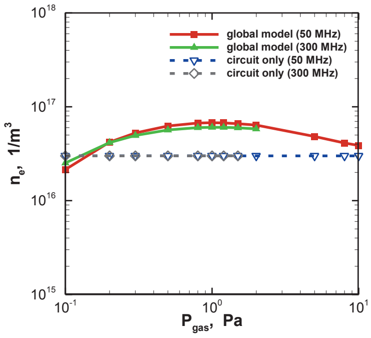

Figure 13. The electron density with neutral gas pressure.

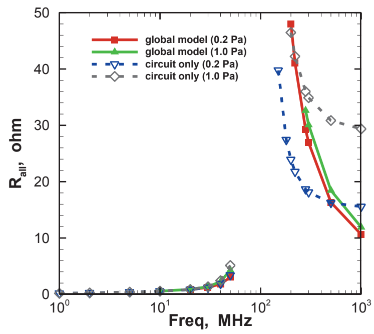

Figure 14. The entire resistance.

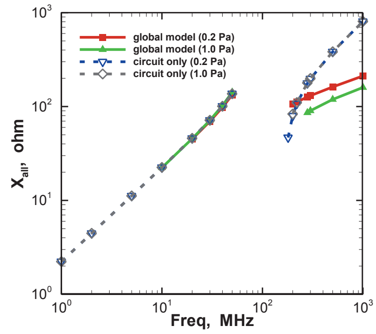

Figure 15. The entire reactance.

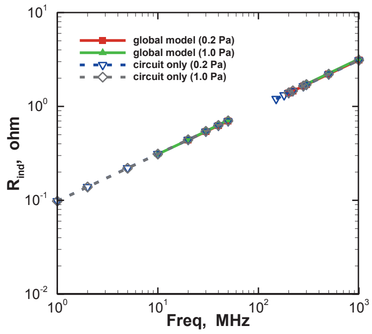

Figure 16. The inductive resistance.

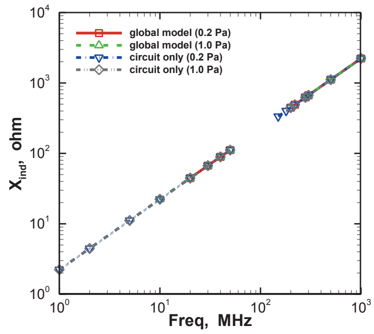

Figure 17. The inductive reactance.

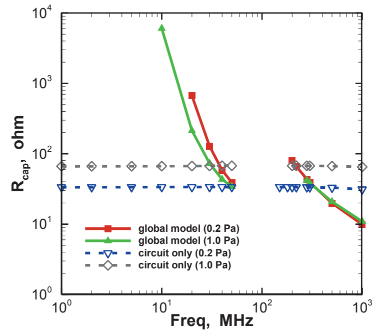

Figure 18. The capacitive resistance.

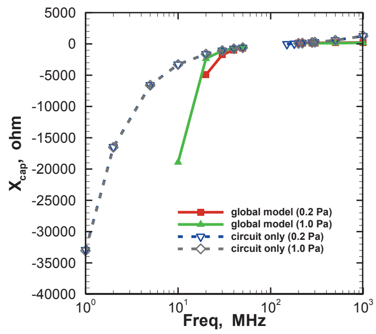

Figure 19. The capacitive reactance.

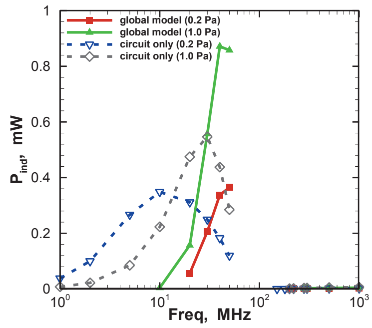

Figure 20. The inductive absorbed power.

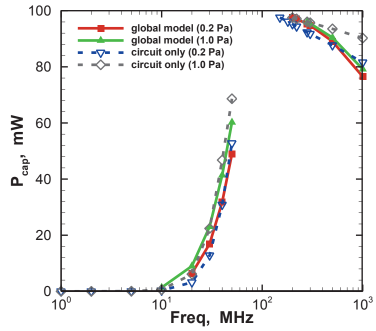

Figure 21. The capacitive absorbed power.

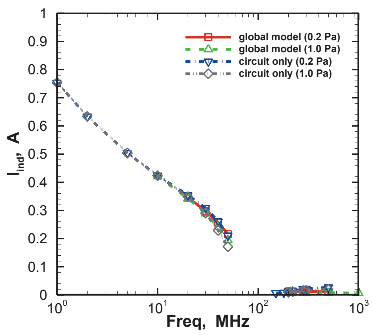

Figure 22. The inductive current.

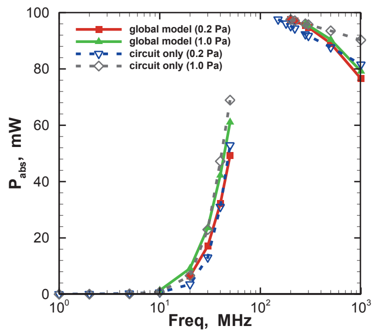

Figure 23. The total absorbed power.

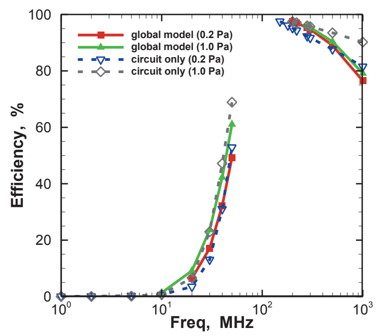

Figure 24. The efficiency.

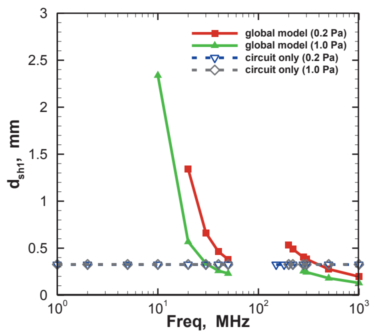

Figure 25. The sheath thickness on the sidewall.

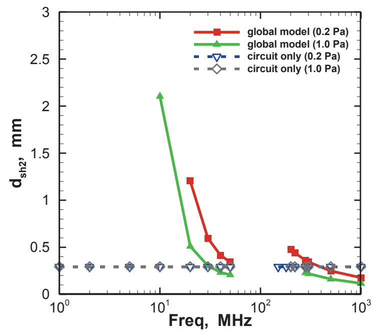

Figure 26. The sheath thickness on the ground.

B. Evaluating The Sheath Resistance on The Sidewall Included Circuit Model

From discussing the sheath thickness, we found that the sheath thickness cannot be ignored. However, in past and this studies, the sheath resistance on the sidewall is ignored because it is estimated to be very small. In this section, the part of capacitive circuit model is changed from figure.7 to figure.27 to include the sheath resistance R_{sh1} due to collisionless stochastic process like R_{sh2} . We describe that the result of calculated this model, again.

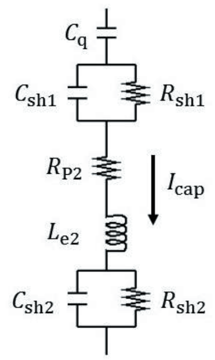

Figure 27. The CCP circuit including $\mathbf{R_{sh1}}$

1. Impedance Frequency Characteristic

Figure.28 and 29 show the resistance and reactance of the discharge chamber and the transmission line as a function of RF frequency. There is not difference in the reactance, but in the lower frequency, the resistance included the sheath resistance on the sidewall is much more than that of neglected it. The result of the inductive and capacitive impedances is shown by figure.30-33. Like V-A, the inductive impedance does not depend on whether including the sheath resistance on the sidewall or not. On the other side, there are differences about the inductive resistance and reactance in the lower frequency. Especially, the capacitive reactance which is including the sheath resistance is much more than that of not included in the lower frequency.

2. Absorbed Power and Efficiency

Figure.34 and 35 show the inductive and capacitive absorbed power as a function of RF frequency. Both of them has only the difference in the lower frequency. However, we confirmed that the total absorbed power is also dominated by capacitive, which is shown by figure.36.

From the same reason in V-A-3, the tendency of efficiency as a function of RF frequency which is shown is figure.37 is similar to that of the total absorbed power. In the higher frequency there is no more difference, but including the sheath resistance on the sidewall, the efficiency in the lower frequency is improved. That is why we consider that there is the difference of the capacitive reactance.

3. Sheath

Figure.38 and 39 show the sheath thickness on the sidewall and on the ground. Both of them has the difference between included the sheath resistance on the sidewall or not in the lower frequency. One of the reason is changing the tendency of the electron density in the lower frequency (figure.40).

From figure.34, in the lower frequency there is a big difference between the two conditions.

Figure.41 shows the sheath resistances on the sidewall and on the ground, and figure.42 shows the ratio of the sheath resistances. The sheath resistances are decreasing with increasing RF frequency but the ratio is about 0.3. Hence, the sheath resistance on the sidewall cannot be neglected to that on the ground.

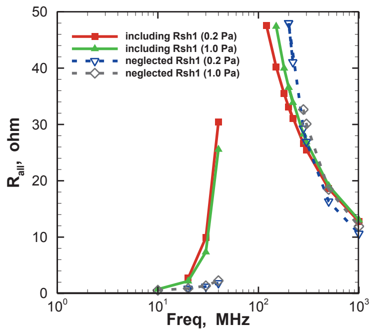

Figure 28. The entire resistance.

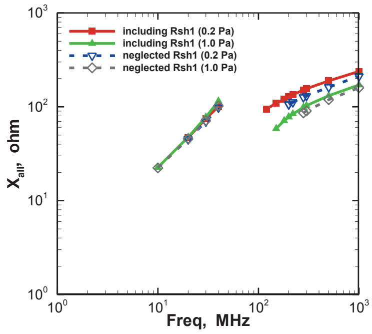

Figure 29. The entire reactance.

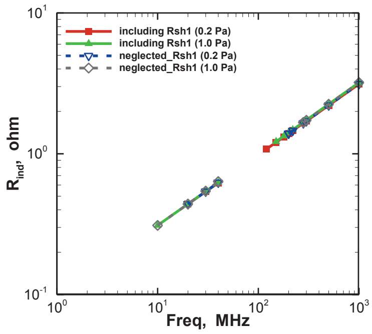

Figure 30. The inductive resistance.

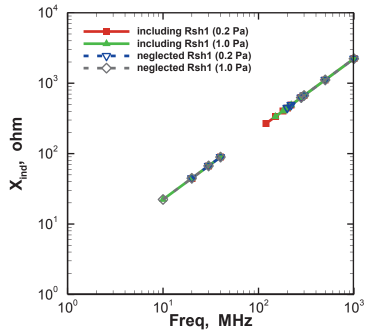

Figure 31. The inductive reactance.

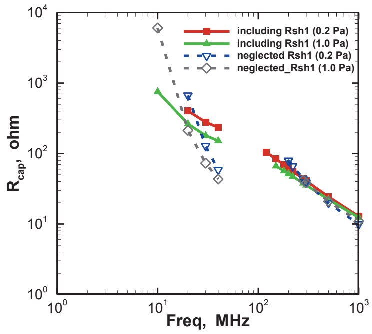

Figure 32. The capacitive resistance.

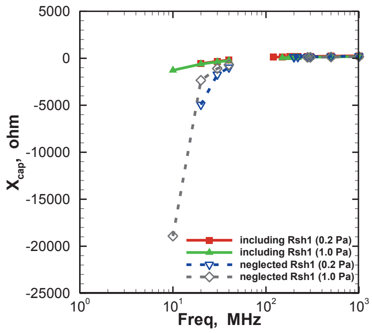

Figure 33. The capacitive reactance.

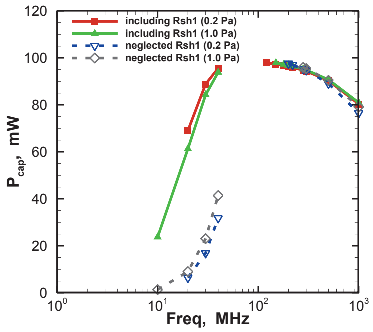

Figure 34. The capacitive absorbed power

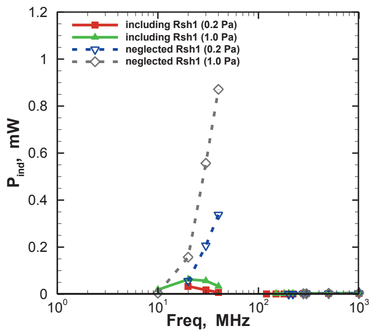

Figure 35. The inductive absorbed power.

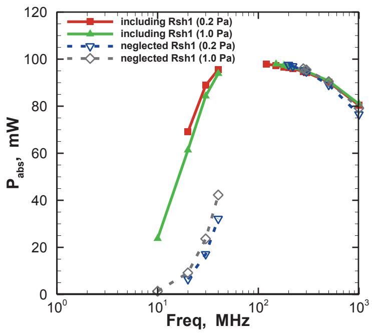

Figure 36. The total power absorbed.

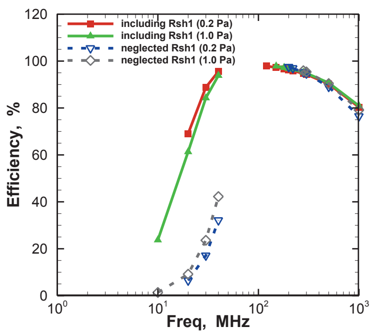

Figure 37. The total efficiency.

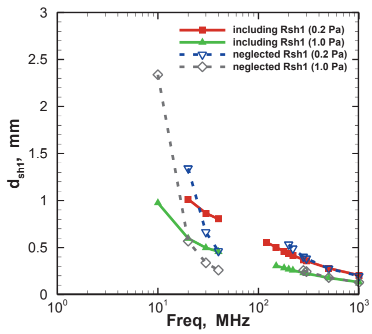

Figure 38. The sheath thickness on the sidewall.

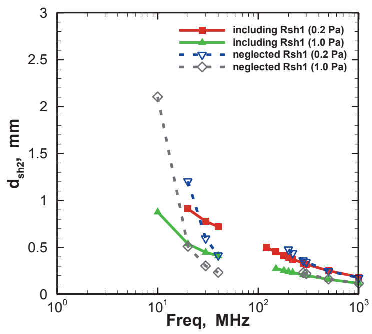

Figure 39. The sheath thickness on the ground.

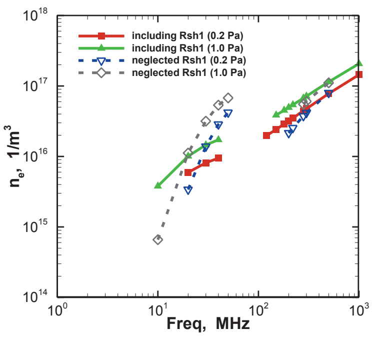

Figure 40. The electro density.

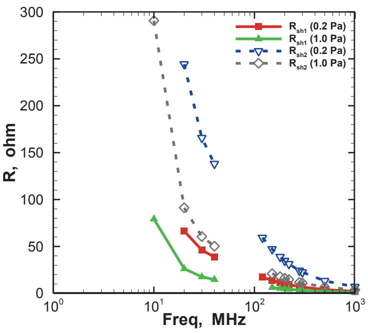

Figure 41. The sheath resistance, including the sidewall sheath resistance.

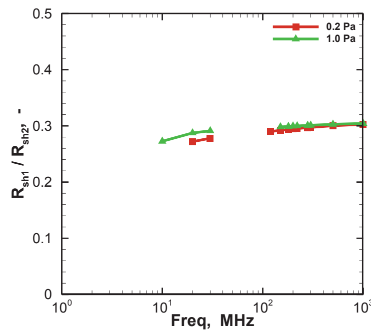

Figure 42. The ratio of the R_{sh1} to R_{sh2}

VI. Conclusion

In this study, we conducted the analysis on mRIT by the equivalent circuit model and the global model. First, we evaluated the influence included the global model. We confirmed that the electron density and temperature has the dependency on the RF frequency and the neutral gas pressure. For this, because the variable of this simulation model can be controlled in experiments, we could say that this model become to be easily to compare to the result of experiments. Furthermore, to investigate the sheath thickness, it was difficult we found that the sheath resistance on the sidewall which was neglected in the past studies could not be neglected.

Second, we evaluated the sheath resistance. Then the ratio of the sheath resistance on the sidewall to the resistance on the ground is about 0.3, in the lower frequency, it is 10% that the percentage of the sheath resistance on the sidewall to the capacitive is. From above, we conclude that the sheath resistance on the sidewall is not able to be ignored. Especially in the lower frequency, from figure.37, included this sheath resistance, we find that the efficiency is more than twice as much as when ignored that. Between 20 - 800 MHz the efficiency is over 80%, and more, between 40 - 200 MHz the efficiency is over 95%.

But around 100 MHz, we cannot calculate this model because the resistance of the discharge chamber and the transmission line is more than 50 Ω, so it is impossible to set the capacitor in matching network.

As a next step, the circuit elements change from lumped constant element to distributed constant because in this frequency band, generally speaking, it is difficult to ignore the electrical wavelength.

Acknowledgments

This works is supported by Dr. Y Takao. And the computer simulation was performed on the KDK computer system at Research Institute for Sustainable Humanosphere, Kyoto University.

References

1) M. M Micci. Micropropulsion for small spacecraft. *American Institute of Aeronautics and Astronautics*, Reston, 2000.

2) H. Yoshiki. Equivalent circuit model of an inductive rf discharge with a helical external coil. *Jpn. J. Appl. Phys*., Vol. vol. 39, no. Part 1, No. 2A, p. 598601, 2000.

3) Michel A.Lieberman. *Principle of Plasma Discharges and Material Processing*. Wiley, 2005

4) F. Iza and J. Hopwood. Influence of operating frequency and coupling coefficient on the efficiency of microfabricated inductively coupled plasma sources. *Plasma Sources Sci. Technol,* Vol. vol. 11, no. 3, p. 229235, 2002.

5) Y. Takao, M. Sakamoto, K. Eriguchi, and K. Ono. Investigation of plasma characteristics and ion beam extraction for a micro rf ion thruster. *Trans. JSASS Aerospace Tech. Japan,* Vol. 12, No. ists29, pp. Pb 13-Pb 18., 2014.